JOURNAL OF VIROLOGY, Oct. 1997, p. 7461–7469 Vol. 71, No. 10
0022-538X/97/$04.00+0

Characterization of Engineered Hepatitis C Virus NS3 Protease Inhibitors Affinity Selected from Human Pancreatic Secretory Trypsin Inhibitor and Minibody Repertoires

NAZZARENO DIMASI,[1] FRANCK MARTIN,[1] CINZIA VOLPARI,[1] MIRKO BRUNETTI,[2] GABRIELLA BIASIOL,[2] SERGIO ALTAMURA,[3] RICCARDO CORTESE,[1] RAFFAELE DE FRANCESCO,[2] CHRISTIAN STEINKÜHLER,[2] AND MAURIZIO SOLLAZZO[1]*

Departments of Biotechnology[1] and Biochemistry[2] and Biotesting Unit,[3] Istituto di Ricerche di Biologia Molecolare P. Angeletti, 00040 Pomezia, Rome, Italy

Received 7 April 1997/Accepted 17 June 1997

Given the extent of hepatitis C virus (HCV) infection as a worldwide health problem and the lack of effective treatment, the development of anti-HCV drugs is an important and pressing objective. Previous studies have indicated that proteolytic events mediated by the NS3 protease of HCV are fundamental to the generation of an active viral replication apparatus, as unequivocably demonstrated for flaviviruses. As a result, the NS3 protease has become a major target for discovering anti-HCV drugs. To gain further insight into the biochemical and biophysical properties of the NS3 enzyme binding pocket(s) and to generate biological tools for developing antiviral strategies, we decided to engineer macromolecular ligands of the NS3 protease domain. Phage-displayed repertoires of minibodies ("minimized" antibody-like proteins) and human pancreatic secretory trypsin inhibitor were sampled by using the recombinant NS3 protease domain as a ligate molecule. Two protease inhibitors were identified and characterized biochemically. These inhibitors show marked specificity for the viral protease and potency in the micromolar range but display different mechanisms of inhibition. The implications for prospective development of low-molecular-weight inhibitors of this enzyme are discussed.

Hepatitis C virus (HCV), the major etiological agent of non-A, non-B hepatitis (8, 23), is estimated to infect over 100 million people worldwide. Infection can lead to chronic and life-threatening diseases such as liver cirrhosis and primary liver cell carcinoma in a substantial number of infected individuals (7). Immunotherapy for HCV infection is not yet available, and treatment with interferon is effective only in a limited number of patients (47). Given the impact of this disease and the lack of an adequate therapy, there is a compelling need for a deeper understanding of the HCV life cycle and identification of targets for developing effective antiviral treatments. The HCV genome encodes a precursor polyprotein of 3,011 amino acids (9, 20, 42), whose enzymatic cleavage leads to the release of structural proteins and enzymes that are essential to the HCV replication process (15, 17). Proteolytic cleavages downstream of the nonstructural gene 3 product (NS3) are catalyzed by a serine protease contained within the N-terminal region of NS3 (2, 11, 16, 43). Studies carried out with flaviviruses (6) support the hypothesis that inhibition of the NS3 protease activity leads to the production of noninfectious viral particles, making this enzyme one of the main targets for anti-HCV drugs.

NS3 is a multidomain protein of 70 kDa that contains, in addition to the protease domain at its N terminus, an RNA helicase at its C terminus (21). A 20-kDa N-terminal fragment of NS3, in association with the viral polypeptide cofactor, NS4A, is capable of performing all cleavages in both in vitro translation and transfection experiments as efficiently as the 70-kDa multidomain protein (12). Peptide bond hydrolysis mediated by this protease occurs preferentially between Cys and Ser or between Cys and Ala in the substrates cleaved in *trans* and between Thr and Ser in the *cis* event occurring at the NS3/NS4A junction (13, 34, 43). The X-ray structure of the NS3 protease 20-kDa domain, either devoid of cofactor (26) or with the bound NS4A peptide (22), has been determined. These studies confirmed that the NS3 protease domain has a trypsin-like β-barrel fold, and, given the relatively featureless appearance of the substrate binding groove, it was anticipated that the design of low-molecular-weight inhibitors would be extremely challenging (22). In addition, recent biochemical studies carried out with synthetic substrates (45) have confirmed this observation, and therefore it is unlikely that classical-mechanism-based small-molecule inhibitors will succeed in achieving potent and selective inhibition of this enzyme.

Given these difficulties, we decided to explore an alternative route based on affinity selection of macromolecular inhibitors by phage display techniques (37), in the attempt to derive a set of basic rules and useful probes for characterizing the properties of the enzyme's active site. Ultimately, our aim is to use some of the information gained from these studies for the development of small-molecule inhibitors. Furthermore, in consideration of the fact that this enzyme is a component of a large polyprotein and associates with other virally encoded protein domains, it is also important to gain further insight into other potential functional sites present on this enzyme's surface which may be targets for developing protein-protein interaction inhibitors.

In this context, small protein scaffolds onto which functions can be engineered are instrumental in generating conformationally defined structures with potential as pharmacophores (38, 48). In recent years, by displaying mutants of natural proteinaceous inhibitors on filamentous phage, new specificities have been selected with high potency (10, 27, 28, 35, 36, 44). Our recent data have shown that different folds such as

* Corresponding author. Mailing address: Department of Biotechnology, Istituto di Ricerche di Biologia Molecolare P. Angeletti, Via Pontina Km 30.600, 00040-Pomezia (Rome), Italy. Phone: 39-6/91093.222. Fax: 39-6/91093.654. E-mail: Sollazzo@IRBM.IT.

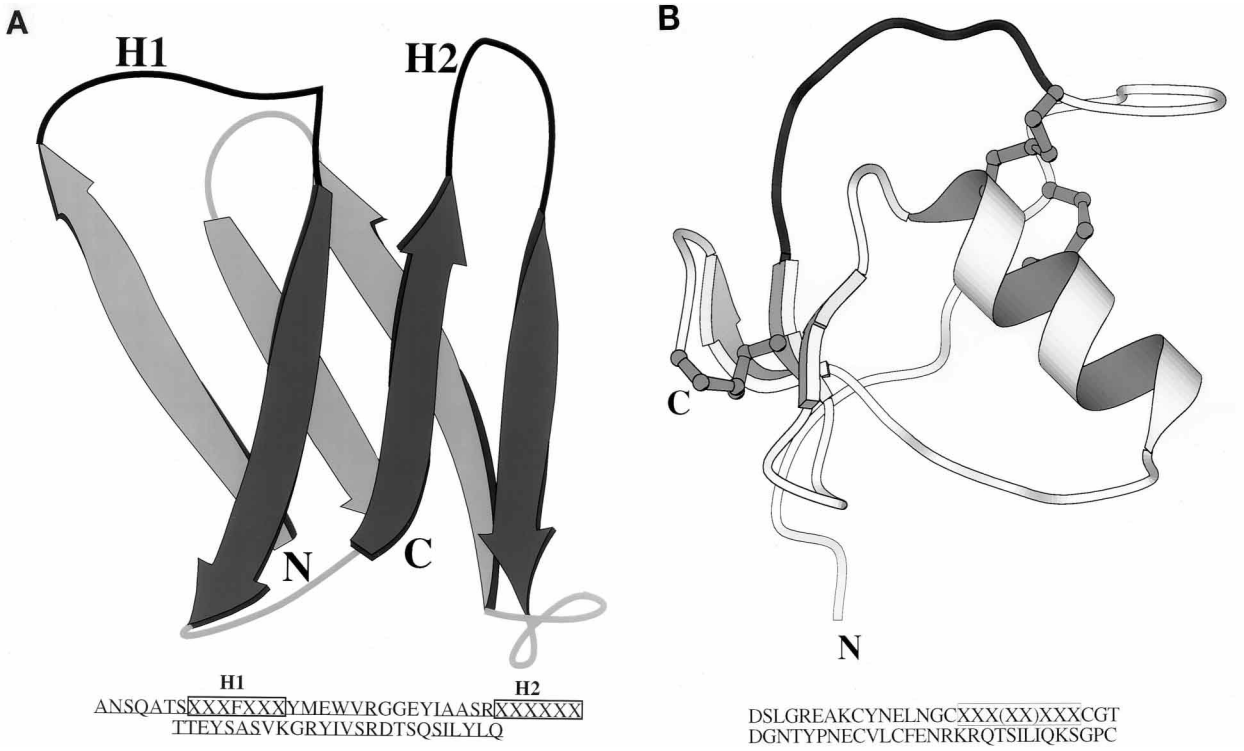

FIG. 1. Schematic representation of inhibitor folding. (A) Amino acid sequence and structural model of the minibody (33). Positions of the hypervariable loops are boxed; β-strands are underlined. In the model the randomized loops are represented as solid black lines and indicated as H1 and H2, whereas β-strands are symbolized by arrows. The amino (N) and carboxy (C) termini are indicated. (B) Ribbon diagram and amino acid sequence of wild-type hPSTI. The randomized binding loop is shown as a dark gray line; disulfide linkages are also shown.

camelized V_H domains are suitable for generating inhibitors of NS3 proteinase activity (31). In order to broaden our analysis and compare the properties of different structural motifs, we decided to expand the panel of diverse protein scaffolds as a source of potential inhibitors. We focused on a repertoire of minibodies ("minimized" β-pleated proteins [29, 33]), with the intention of probing β-turn structural motifs (Fig. 1A). In addition, following the rationale of other authors (35, 36), we sampled a second repertoire derived from the natural Kazal-type serine protease inhibitor (Fig. 1B), human pancreatic secretory trypsin inhibitor (hPSTI).

We report here the affinity selection and characterization of two inhibitors of HCV NS3 protease from repertoires of the above-mentioned macromolecular scaffolds. These molecules—MBip, a noncompetitive minibody inhibitor, and hPSTI-C3, a competitive inhibitor—provide clues about the structural requirements for achieving effective enzymatic inhibition. We discuss the impact that these results and reagents may have in the development of anti-HCV compounds.

MATERIALS AND METHODS

Microbiological and recombinant DNA techniques. Microbiological and recombinant DNA techniques were carried out according to standard protocols (1) or as recommended by suppliers. Oligonucleotides were synthesized by using an Applied Biosystems (Foster City, Calif.) 380B synthesizer. Phage manipulations and *Escherichia coli* electroporation were carried out as described previously (29).

Construction, expression, and partial purification of NS3-Myc protease. The construction, expression, and purification of NS3-Myc (strain Bk NS3 protease domain from residue 1027 to residue 1206), in which the Myc epitope (EFEQKLISQQDLG) is fused to the C terminus of the protease, were described previously (31). The protease-containing solution was made 50% in glycerol content and kept at −20°C until used.

NS3 protease assays. Assays were performed in 50 mM Tris (pH 7.5)–2% CHAPS {3-[(3-cholamidopropyl)-dimethylammonio]-1-propanesulfonate} and in the presence of either 50% glycerol and 30 mM dithiothreitol (DTT) (for all experiments with the minibody) or 15% glycerol and 0.1 mM DTT (for all experiments with hPSTI). The enzyme, i.e., the NS3 protease 20-kDa domain purified from *E. coli* (40), was used at concentrations ranging from 10 to 150 nM. The protease was preincubated for 15 min with a 14-mer peptide corresponding to the central domain of the protease cofactor NS4A containing the sequence GSVVIVGRIILSGR (44). To 60 μl of assay mix, up to 6 μl of inhibitor solutions (or corresponding amounts of buffer) was added, and incubation was continued for a further 30 min at 25°C. Reactions were started by adding 40 μM substrate peptide acetyl-DEMEECASHLPYK-NH_2 and stopped by adding 40 μl of 1% trifluoroacetic acid (TFA) at <20% conversion. Samples were analyzed by high-pressure liquid chromatography (HPLC) with a Merck-Hitachi chromatograph equipped with an autosampler, column oven, and fluorescence detector. Samples (45 to 90 μl) were injected on a reversed-phase HPLC cartridge column (C_{18} Lichrospher; 5 μm, 0.4 by 7.5 cm [Merck]) equilibrated with 90% H_2O–0.1% TFA (solvent A) and 10% acetonitrile–0.08% TFA (solvent B) and operating at a flow rate of 2.5 ml/min. A 10 to 40% gradient of solvent B at 5%/min was used to separate cleavage fragments. Peaks were detected by monitoring tyrosine fluorescence (excitation at 260 nm and emission at 305 nm). Cleavage products were quantified by integration of chromatograms with reference to samples in which 100% conversion was achieved by 12 h of incubation in the presence of 2 μM protease.

Fifty percent inhibitory concentrations (IC_{50}s) were calculated by fitting inhibition data to equation 1 by using Kaleidagraph software:

$$\% \text{ activity} = \text{maximum activity}/\{1 + ([I]/IC_{50})^S\} \quad (1)$$

where [I] is the inhibitor concentration, maximum activity is the enzyme activity in the absence of inhibitor, and S is the slope factor of the curve.

Reversibility of inhibition was assessed by dilution experiments. Briefly, NS3 protease was preincubated with inhibitor at a concentration of 4 to 5 times the IC_{50} as described above. After 30 min, half of the sample was diluted 10-fold, and activities in both samples were determined and compared to the activities in a sample incubated with a buffer blank and a sample incubated from the beginning with a 10-fold-diluted inhibitor. Inhibition was defined as reversible if more than 75% of activity was recovered upon dilution.

Inhibition mechanisms were determined by performing substrate titration

experiments using concentrations of substrate peptide of between 15 and 250 μM (K_m/3.3 and 5 × K_m) in the absence and in the presence of different inhibitor concentrations. Initial rates of cleavage were determined for samples with <20% conversion. Double-reciprocal plots (1/*V* versus 1/*S*) were used to visualize inhibition mechanisms. Kinetic parameters were calculated from least-squares fits of initial rates as a function of substrate concentration with the help of Kaleidagraph or Sigmaplot software, assuming Michaelis-Menten kinetics. K_i and K_{ii} values were calculated by refitting the data to a modified Michaelis-Menten equation (equation 2):

$$V = V_{max}S/\{K_m(1 + [I]/K_i) + S(1 + [I]/K_{ii})\} \quad (2)$$

Affinity selection. The library used for affinity selection was described earlier (29). Briefly, the library was constructed by inserting randomized (NNG/T) oligonucleotides in the region corresponding to the H1 and H2 loops of the prototype minibody molecule shown in Fig. 1A. The library contained a total of approximately 5×10^7 transformants. The design of the pSKAN-8 library was described previously (36), and the library was purchased from MoBiTec, Göttingen, Federal Republic of Germany. The library has a complexity of about 10^8 variants whose binding loop was randomized both in length (six to eight residues) and sequence. Selections were carried out as described before (31), except for the amplification of the hPSTI library, which was carried out in the WK6λmutS host (36) instead of K91 cells. The selection buffer was 15% glycerol–0.1 mM DTT–50 mM NaCl–0.5% CHAPS–10 mM Tris-HCl (pH 7.5).

Western blot analysis. Western blot analysis of phagemid preparations was carried out by collecting phage particles by polyethylene glycol precipitation and separating proteins by sodium dodecyl sulfate–10% polyacrylamide gel electrophoresis (SDS–10% PAGE). Following electrotransfer onto a polyvinylidene difluoride filter, the blot was incubated with anti-pIII serum for 1 h at room temperature and revealed with peroxidase-conjugated antirabbit antibodies.

Expression and purification of minibody and hPSTI. High levels of minibody expression were achieved by using the PT_7 promoter as described previously (3, 29). The PCR primers used were T7up (5′-ATATACATATGGCTAACTC CCAG-3′) and T7dwn (5′-GGAACCCTGCAGATACAGGATG-3′). The protein concentration was determined by amino acid analysis.

The constructs expressing hPSTI-C3 and wild-type hPSTI carrying His_6 and FLAG epitopes at their C termini were transformed in *E. coli* GC383 bearing the plasmid pcI857 (19), which expresses a temperature-sensitive repressor product of the phage lambda gene *c*I (a kind gift of G. Cesareni, University of Rome, Rome, Italy). These expression vectors were obtained by modifying the pMAC8 vector described earlier (41), using standard recombinant DNA techniques. The tag encoding the epitope A3C5 in pMAC8 was replaced with the synthetic FLAG epitope constructed by using the complementary oligonucleotides hPSTIup (5′-CATGGTTTCGACTACAAAGACGACGACGACAAATA-3′) and hPSTIdwn (5′-AGCTTATTTGTCGTCGTCGTCTTTGTAGTCGAAAC-3′). The fragment was cloned at the *Nco*I/*Hin*dIII sites of pMAC8, thus creating pMAC9, which in turn was used as a host vector for cassette insertions (at the unique *Sal*I and *Kpn*I sites) of DNA fragments encoding the amino acid sequences of selected clones. The hPSTI3 oligonucleotide (5′-GGAGGTCTAGATAACG AGA-3′) was used as a sequencing primer. Cells were grown in Luria-Bertani medium at 28°C to an optical density at 600 nm (OD_{600}) of 0.8, heat shocked to 42°C to induce protein expression, and harvested 6 h later by centrifugation. The wild-type hPSTI was purified from periplasmic extract, under native conditions by immobilized metal affinity chromatography (IMAC) (18) followed by a gel filtration step, whereas the hPSTI-C3 protein was purified by the same protocol but under denaturing conditions (6 M urea and 100 mM DTT). Renaturation and concomitant reoxidation of reduced protein was performed by extensive dialysis (30 h at 4°C) against 0.05 M Tris-HCl (pH 8)–1 M urea–0.05% Tween 80 containing reduced or oxidized glutathione as an "oxido-shuffling" agent. Empirically we established that the regeneration of native protein disulfide bonds proceeds optimally in the presence of 2 mM reduced glutathione and 0.02 mM oxidized glutathione, as monitored by PAGE under reducing and nonreducing conditions. After this step, the protein was dialyzed against protease buffer (50 mM Tris [pH 7.5], 2% CHAPS, 50% glycerol, 0.1 mM DTT). For the carboxyamidomethylation of the protein we used iodoacetamide (purchased from Sigma) as follows: 15 μM hPSTI-C3 in 200 μl of buffer containing 2% CHAPS, 0.1 mM DTT, 0.05 mM Tris-HCl (pH 7.5), and 10% glycerol was treated with 50 mM iodoacetamide for 2 h at room temperature in the dark, followed by overnight dialysis against the same buffer without iodoacetamide.

ELISA. Microtiter wells coated with NS3 (10 μg/ml) in 200 mM Tris (pH 8.0) were blocked with 5% nonfat dry milk in 10 mM Tris (pH 7.5)–50 mM NaCl–1% CHAPS–10% glycerol–0.1 mM DTT (protease enzyme-linked immunosorbent assay [ELISA] buffer [PEB]). For phage ELISA binding, 10^{11} transducing units (TU) in PEB containing 1% milk were added and incubated overnight at 4°C. After washing with 50 mM Tris (pH 7.5)–150 mM NaCl containing 0.05% Tween 20, plates were incubated with a 1:7,000 dilution of rabbit antiphage antibodies (14), and the complex was revealed with alkaline phosphatase (AP)-conjugated antirabbit antibodies (1:7,000). The AP activity was determined with the soluble chromogenic substrate, and the OD_{405} was recorded after 15 to 60 min of incubation at 23°C. For the competition experiments the NS3 protease was added to a final concentration of 1 μM. The direct binding assay with purified proteins was carried out as previously described (29) except that the buffer was PEB with 1% milk and the polypeptides were tested at 2 μM.

Gel filtration chromatography. Gel filtration experiments were performed with a Pharmacia fast protein liquid chromatography system on a Superdex-75 analytical or preparative column equilibrated in 50 mM Tris buffer (pH 7.5) containing 10% glycerol, 2 mM DTT, and 1% CHAPS. The calibration run was done with the Pharmacia Biotech LMW gel filtration calibration kit, which includes the markers dextran blue, bovine serum albumin (BSA), ovalbumin, chymotrypsinogen, RNase, and aprotinin, corresponding to 200, 67, 43, 25, 13.7, and 6.5 kDa, respectively.

In vitro translation of NS3 (70 kDa) and substrate. DNA fragments derived from HCV strain Bk cDNA were inserted downstream of the 5′ untranslated region of encephalomyocarditis virus, under control of the T7 promoter in the pCite-1 vector (Novagen) in the appropriate translational reading frame and followed by a termination codon. The plasmids pCiteNS3-4AΔcut and pCiteNS5ABΔC51, expressing, respectively, the HCV proteins NS3-4A (residues 911 to 1711) with a mutated cleavage site and NS5AB (residues 1965 to 2471), were previously described (39, 44). In vitro transcription was done with T7 RNA polymerase (Promega). The transcripts were translated for 1 h at 30°C in the presence of [^{35}S]methionine with RNA-dependent rabbit reticulocyte lysate (Promega). Cleavage of the labelled precursor was assessed by SDS-PAGE on 12.5% gels and exposure on a PhosphorImager (Molecular Dynamics).

Elastase, kallikrein, and trypsin assays. Pancreatic porcine elastase, its substrate (Me-*o*-Suc-Ala-Ala-Pro-Val-pNA), and pancreatic porcine kallikreine were purchased from Calbiochem. The pancreatic porcine kallikreine substrate Chromozym was purchased from Boehringer Mannheim. The pancreatic porcine elastase assay was performed in a 96-well plate in 50 mM Tris (pH 7.5)–500 mM NaCl–0.05% Triton X-100–5% dimethyl sulfoxide buffer; the enzyme and substrate were added to final concentrations of 0.5 μg/ml and 500 μM, respectively. Samples were tested in a 100-μl final volume, and after 75 min of incubation at room temperature under constant agitation, the OD_{405} was recorded. The pancreatic porcine kallikreine assay was performed in 50 mM Tris (pH 8)–0.01% Triton X-100–5% dimethyl sulfoxide; the concentrations of the protease and its substrate were 50 nM and 100 μM, respectively. After 1 h of incubation at 23°C under agitation, the OD_{405} was recorded. For the trypsin assay, the proteins were incubated with 0.42 pmol of trypsin in 0.5 ml of 0.2 M Tris-HCl buffer (pH 8.0) containing 0.02% NaN_3 and 0.05% Tween 80 for 5 min at 25°C. Next, 0.1 ml (160 nmol) of the substrate *N*-benzolyl-L-Ile-L-Glu-L-Ile-L-Gly-L-Arg-*p*-nitroanilide (in 0.1 M Tris-HCl [pH 8.0]–0.01% NaN_3–0.025% Tween 80–15% ethanol) was added to the mixture. Trypsin-inhibitory activity was determined by measuring the OD_{405}. Calibration curves were made by using aprotinin as a standard.

RESULTS

In order to carry out affinity selection of macromolecule repertoires displayed on filamentous phage, we used the modified 20-kDa N-terminal fragment of NS3 protease described previously (31). This protein has the Myc tag epitope (EFEQKLISQQDLG) fused to its C terminus to enable its immobilization onto a solid-phase matrix in a bioactive conformation. For a source of ligands, we aimed at sampling two previously described repertoires that were constructed as fusions with the f1 phage pIII minor coat protein: namely, an hPSTI library in which the binding loop was randomized in both length (six to eight residues) and sequence (36) and a minibody library in which the H1 and H2 regions (six residues each) were randomized (29). The hPSTI library was constructed in a monovalent display format (phagemid vector), whereas the minibody library was made as a multivalent system (phage vector).

Two and five rounds of selection were carried out with the minibody and hPSTI repertoires, respectively. Subtractive steps, consisting of incubation of the amplified library with the matrix, including all reagents but without the NS3 20-kDa domain, were included between rounds as reported before (29). Because NS3 protease requires detergent and kosmotropic agents for optimal activity (39), affinity selection steps were carried out in the presence of 15% glycerol and 1% CHAPS detergent for 4 h at room temperature under mild reducing conditions (0.1 mM DTT in an N_2 atmosphere). We chose these experimental conditions to maintain an adequate environment for enzymatic activity and at the same time avoid disruption of the hPSTI disulfide linkages, as shown previously (31).

TABLE 1. Amino acid sequences of the hPSTI loops of affinity-selected phage ligands

hPSTI	Variable region	No. of isolates in round:	
		4	5
Wild type	CTKIYDPVC		
hPSTI-C1	CGVACKAVC	2	7
hPSTI-C2	CESDCDYGC	1	5
hPSTI-C3[a]	CWHACRRVC	2	1
hPSTI-B8	CGESPNEVC		6
hPSTI-A6[a]	CWVKEELWQC	1	8
hPSTI-A14	CCRGCDAGGC	1	
hPSTI-A16	CRCRDASKNC	2	
hPSTI-A17	CDTRDRMRWC		4
hPSTI-A21	CSCGAEHGEC		2
hPSTI-A23	CECLVGWGVC		3

[a] Construct that yielded a detectable amount of protein in the bacterial periplasmic space.

Following selection steps, phage clones from the fourth and fifth rounds of hPSTI panning (total of 46) and from the second round of minibody panning (total of 48) were cultured and concentrated by polyethylene glycol precipitation. The single-stranded DNA was extracted from phage preparations, and the amino acid sequence of the randomized region was deduced from DNA sequences. Many of the hPSTI clones were multiple isolates of the same variant, and remarkably, about 70% of them possess a cysteine residue in the protease binding loop (Table 1). Interestingly, cysteine is the preferred P1 side chain for optimal NS3-mediated cleavage. For the minibody selection the outcome was clearly different (see below).

We tested the phage supernatants by direct binding on NS3-coated ELISA plates with a rabbit antiphage serum as the revealing reagent (phage ELISA). Of the 48 minibody phage clones analyzed, 14 scored positive in this binding assay (the amino acid sequences of their H1 and H2 regions are shown in Table 2). Five clones in particular showed a significant signal/noise ratio on the NS3 protease- as opposed to BSA-coated wells (Fig. 2A). The outcome is different from that with hPSTI, as no clear consensus emerged and all isolates were single, except for one clone that turned out to have the highest signal in the phage ELISA. In addition, only two isolates have cysteine residues in their variable region. This difference may reflect either the limited complexity of the minibody repertoire sampled and/or the minimal number of amplification steps carried out (see Discussion). The same phage ELISA carried out with hPSTI phagemid isolates did not yield a meaningful result. All clones tested, including the wild-type hPSTI, showed high background levels (not shown). Probably the combination of monovalent display, modest affinity, and intrinsic stickiness of hPSTI for the immobilized NS3 makes it impossible to get a clean signal.

The phage-minibodies were tested in a secondary assay where the binding of phage particles to the NS3-coated wells was competed by 1 μM protease in solution phase (Fig. 2B). The rationale for this assay was that if the minibody bound the native NS3 protease in solution phase, its binding to the solid-phase-immobilized enzyme would be competed out by the free ligate. This experiment would delimit a subgroup of phage ligands of those that interact with nonnative conformations of the NS3. Five minibodies displaying this behavior also showed the strongest signals in the phage ELISA direct binding and were characterized further. The genes encoding these bona fide NS3 ligands were amplified by PCR with the phage DNA as a template and an appropriate set of primers. The amplified fragments were subcloned into the pT7 vector for high-level expression in *E. coli*. The minibodies bearing the octameric peptide FLAG (IBI, New Haven, Conn.) genetically fused to the C terminus were expressed, purified, and refolded before further testing.

Because of the impossibility of prescreening the hPSTI mutants isolated (such as by phage ELISA), we decided to go one step forward and use purified proteins instead of phage preparations. To this end, the DNA fragments encoding the variable regions of the isolates shown in Table 1 were excised from the phagemid double-stranded DNA (dsDNA) (by digestion with *Sal*I and *Kpn*I) and subcloned into the pMAC9 vector, which is suitable for expression in the periplasmic space of *E. coli*. Of the 10 constructs tested, only 2 yielded detectable amounts of protein in the bacterial periplasmic space (Table 1), and of these 2, the only protein we were able to refold was the hPSTI-C3 variant. This extremely low rate of productive expression of the hPSTI variants remains to be explained (see Discussion), as it appears that the same mutants expressed as pIII fusion proteins were clearly detectable on the phage surface (Fig. 3). The hPSTI-C3 variant was purified by IMAC (18) and gel filtration before testing.

Figure 4 shows the binding of the purified minibody ligands chosen and of hPSTI-C3 to HCV NS3 protease applied to microtiter wells, except for one polypeptide (MBe), whose solubility in aqueous buffers was too low (<4 μM) to be properly analyzed. It should be emphasized that binding is carried out in selection buffer containing 10 mM Tris (pH 7.5), 15% glycerol, 50 mM NaCl, and 0.1 mM DTT. The direct binding assay with purified minibodies confirms the results obtained with the phage ELISA, except for the intensities of the signal in the two assays, which do not always correspond. Differences in the apparent potency could be due to multimerization of the ligands on the phage surface, thus giving rise to avidity effects that can result in an apparently higher level of binding. Also, hPSTI-C3 appears to bind to solid-phase-immobilized NS3, although the wild-type hPSTI appears to bind to the immobilized enzyme, albeit to a lower degree.

Next, we asked whether any of these NS3 binders were also inhibitors of enzymatic activity. As a preliminary screen for inhibition activity, we tested these purified molecules at a sin-

TABLE 2. Amino acid sequences of the H1 and H2 regions of affinity-selected NS3 phage ligands

Minibody	H1 region[a]	H2 region
Wild type	GFTFSDF	NKGNKY
MBa	TQAFLNM	NKGNKY
MBb[b]	KSTFGWD	LCRTIG
MBip	WRLFYAE	GWEASR
MBc	EGRFWYR	NKGNKY
MBd	SYIFRSS	NKGNKY
MBe	RYRFLGQ	NKGNKY
MBf	GIDFRRF	GSLVVI
MBg	REPFSCP	NKGNKY
MBh	WDAFEAW	NKGNKY
MBi	GFTFSDF	SDFEAS
MBj	YSRFRGK	NKGNKY
MBl	GTWFPRD	NKGNKY
MBns[c]	GFTFSDF	DLHSND

[a] The central phenylalanine in the H1 regions is an invariant residue in the minibody library (30).
[b] Found three times.
[c] Nonselected minibody.

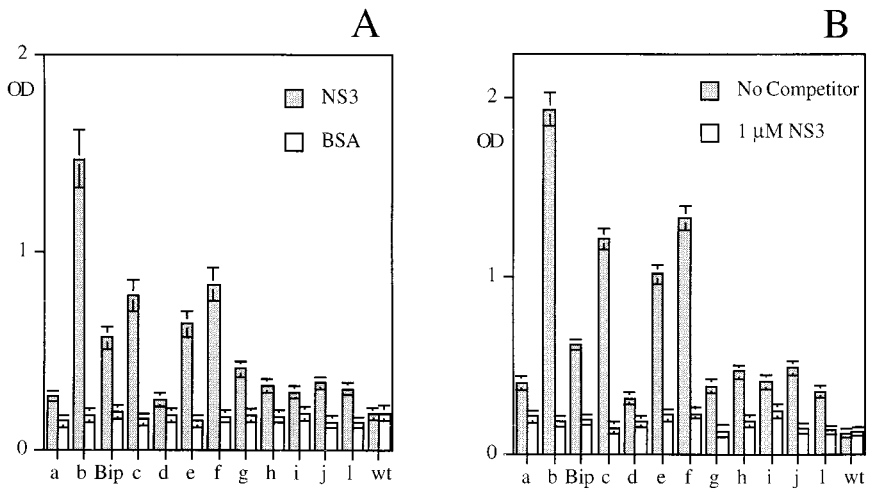

FIG. 2. Phage ELISA binding of minibodies to NS3. (A) Direct binding of the selected phage-minibodies (10^{11} TU/well) to solid-phase-immobilized NS3 or BSA on 96-well ELISA plates. The phage-bound particles were detected by using an anti-pVIII rabbit serum and AP-conjugated antirabbit antibodies. (B) Competition of the phage-minibodies (10^{11} TU/well) for binding to immobilized NS3 with 1 μM soluble protease. OD_{405}s are recorded, and data are the averages and standard deviations for triplicate samples in both experiments. wt, wild type.

gle concentration (the highest possible) in the protease activity assay. We carried out this assay by monitoring residual enzyme activity in the presence of inhibitors by using a small fluorescent substrate at a concentration of 40 μM. In this experiment only one of the minibody ligands (MBip) and hPSTI-C3 scored as inhibitors of the protease activity (not shown). High concentrations (up to 40 μM) of wild-type hPSTI and a nonselected minibody (MBns) do not produce any significant levels of enzyme inhibition. Because of their evident inhibition activity, we decided to perform additional characterization of hPSTI-C3 and MBip.

To accurately estimate the potencies of these inhibitors, we carried out titration experiments of enzymatic activity as a function of inhibitor concentration by using the same assay as described above. The IC_{50}s of hPSTI-C3 and MBip were estimated to be 540 and 1,500 nM, respectively (Fig. 5). It is important to note that all experiments with MBip, including the determination of its IC_{50}, were carried out under optimal assay conditions for NS3 protease activity (50% glycerol and 30 mM DTT), whereas all hPSTI tests were performed under suboptimal conditions (15% glycerol and 0.1 mM DTT). Glycerol concentrations of above 15% inhibit the binding of hPSTI-C3 to NS3, and a high concentration of DTT causes it to unfold. Because hPSTI-C3 and MBip activities were not inhibited by the NS4A cofactor peptide and vice versa, it appears that the selected ligand can bind both forms of the enzyme, as a free species and as a heterodimer complex.

It was also important to establish the reversibility of the two inhibitors. We assessed reversibility by using an assay in which the enzyme was preincubated with 3 and 7.5 μM hPSTI-C3 and MBip inhibitors, respectively (five times their IC_{50}s), followed by a 10-fold dilution and determination of the residual enzymatic activity (data not shown). The results were consistent with reversible inhibition for both molecules, as we recovered more than 80% of the enzyme activity upon dilution of the complex.

In order to rule out possible artifacts due to nonspecific aggregation of the selected polypeptides, we carried out gel

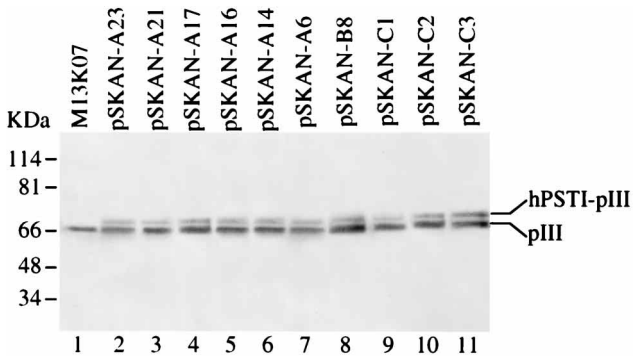

FIG. 3. Western blot of hPSTI phagemid mutants. Phagemid particles (10^{11} TU/lane) of selected clones were subjected to SDS–10% PAGE and transferred to polyvinylidene difluoride filters. Blots were stained with rabbit anti-pIII serum followed by AP-conjugated antirabbit antibodies.

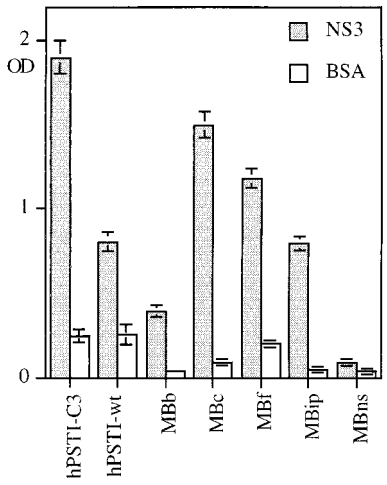

FIG. 4. Direct binding assay. ELISA direct binding of purified minibodies (2 μM) and hPSTI-C3 (1 μM) polypeptides to NS3- or BSA-coated wells. The bound proteins were detected by using the anti-FLAG monoclonal antibody M2 and an AP-conjugated secondary antibody. OD_{405}s are recorded, and data are the averages and standard deviations of three experimental values.

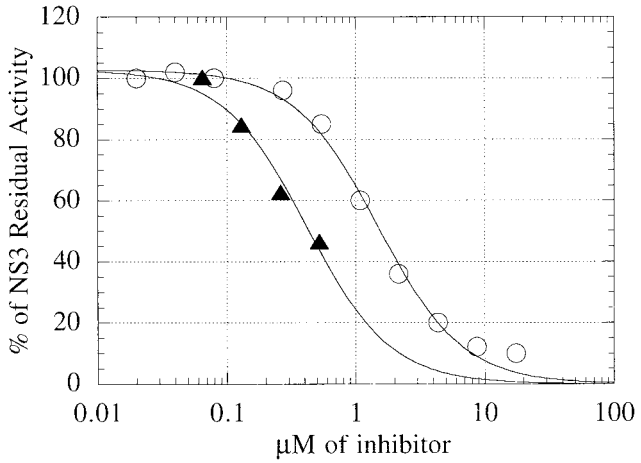

FIG. 5. Determination of IC_{50}. The recombinant NS3 20-kDa fragment protease (20 nM) was incubated in the presence of increasing amounts of purified hPSTI-C3 (triangles) and MBip (circles) inhibitors (averages of duplicate samples), 40 μM substrate, and 3 μM NS4A cofactor. The cleaved peptide substrate concentration was determined by HPLC. The percentage of residual activity (*y* axis) was determined as function of inhibitor concentration (*x* axis), and the IC_{50} was derived.

filtration chromatography (Fig. 6) to assess the apparent molecular weights of both MBip and hPSTI-C3 under assay buffer conditions. The molecules migrate as monomer species with the expected molecular weights in the protease assay buffer, except with the glycerol concentration lowered to 10% (the maximum compatible with fast protein liquid chromatography) and the CHAPS concentration lowered to 1%.

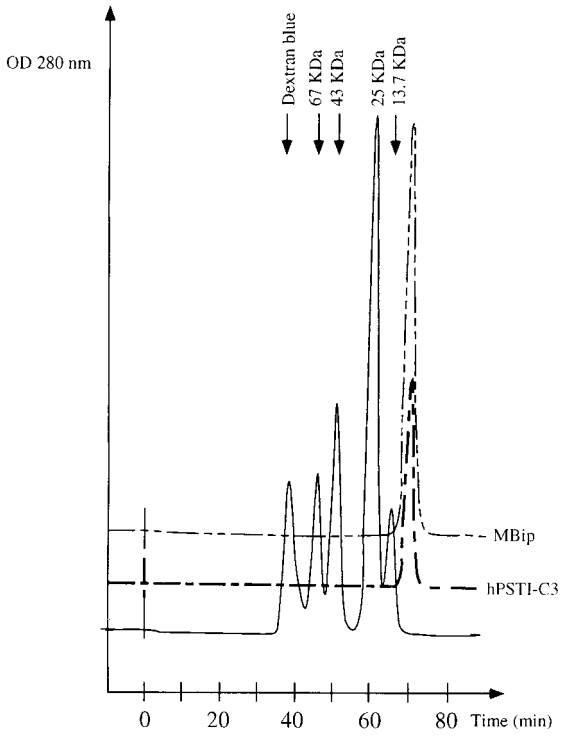

FIG. 6. Gel filtration chromatography. The molecular masses of the purified hPSTI-C3 and MBip proteins were determined by gel filtration. The molecular mass standards are indicated. The retention time for both inhibitors corresponds to the calculated value of a monomer for both proteins.

Next, we checked the specificity of binding by testing both inhibitors in two commercially available serine proteinase assays, namely, those for porcine elastase and kallikrein. Neither of these enzymes was inhibited to any measurable extent upon incubation with NS3 inhibitors at 13 μM (the maximal concentration testable, given their limited solubility), corresponding to a 5- to 30-fold excess of the inhibitor/substrate ratio, thus indicating a substantial level of selectivity. The hPSTI-C3 inhibitor was also tested in a trypsin assay and proved to be inactive.

To establish the mechanism of action of the hPSTI-C3 inhibitor, substrate titration experiments were performed in the absence and in the presence of 0.78 and 1.56 μM hPSTI-C3 (Fig. 7A). By fitting the experimental data to a modified Michaelis-Menten equation (equation 2; see Materials and Methods), the dissociation constants of the enzyme-inhibitor complex (K_i) and of the ternary enzyme-inhibitor-substrate complex (K_{ii}) were determined. We obtained a K_i of 360 nM and a very high value for K_{ii}. This result indicates that the hPSTI-C3 inhibitor binds to the free enzyme but has virtually no affinity for the enzyme-substrate complex, as expected for a competitive inhibitor. Most likely, the selected molecule binds to the enzyme active site by using the free cysteine residue of the protease binding loop as its main specificity determinant. In fact, when we carboxyamidomethylated the cysteine residue with 10 mM iodoacetamide, the hPSTI-C3 protein lost its activity (Fig. 7A, inset). On the other hand, the same experiment carried out with MBip (Fig. 7B) clearly showed that this molecule has a noncompetitive mechanism of inhibition, with a K_i of 1.1 μM and a K_{ii} of 3.9 μM. Most likely, the selected MBip recognized a site that is distinct from both the substrate and NS4A binding sites, as its activity was unaffected by the presence of NS4A. We also verified that hPSTI-C3 and MBip were not cleaved by NS3 after overnight incubation with high concentrations (30 μM) of enzyme (data not shown). This observation demonstrates that the inhibition of NS3 by either molecule was not due to cleavage of a potential alternative substrate.

Finally, because of the lack of cell-based replication systems for HCV, as a surrogate for a biological assay for HCV replication, we determined if hPSTI-C3 and MBip were active on the entire (70-kDa) NS3 gene product (including the helicase domain) and on its natural substrate. In this experiment, hPSTI-C3 (Fig. 8A) inhibited the proteolytic activity of the 70-kDa protein with an apparent IC_{50} of approximately 1.2 μM (twofold greater than the value determined by the activity titration assay), whereas MBip (Fig. 8B) had an apparent IC_{50} of 1 μM, in good agreement with that measured by HPLC titration with the synthetic small substrate.

DISCUSSION

HCV NS3 protease is currently the focus of intensive studies to develop anti-HCV drugs. One important consideration emerged from the structural determination of the NS3 protease domain (22, 26): as a result of the absence of some loops (which are generally well conserved among serine proteinases), the substrate binding site of NS3 is relatively flat and shapeless. Hence, it was anticipated that making substrate-based small-molecule inhibitors would prove a formidable task (22). Further support for this observation emerged from biochemical studies carried out with synthetic substrates (45). It is our opinion that a deeper understanding of the NS3 surface properties and the availability of further biological tools for cocrys-

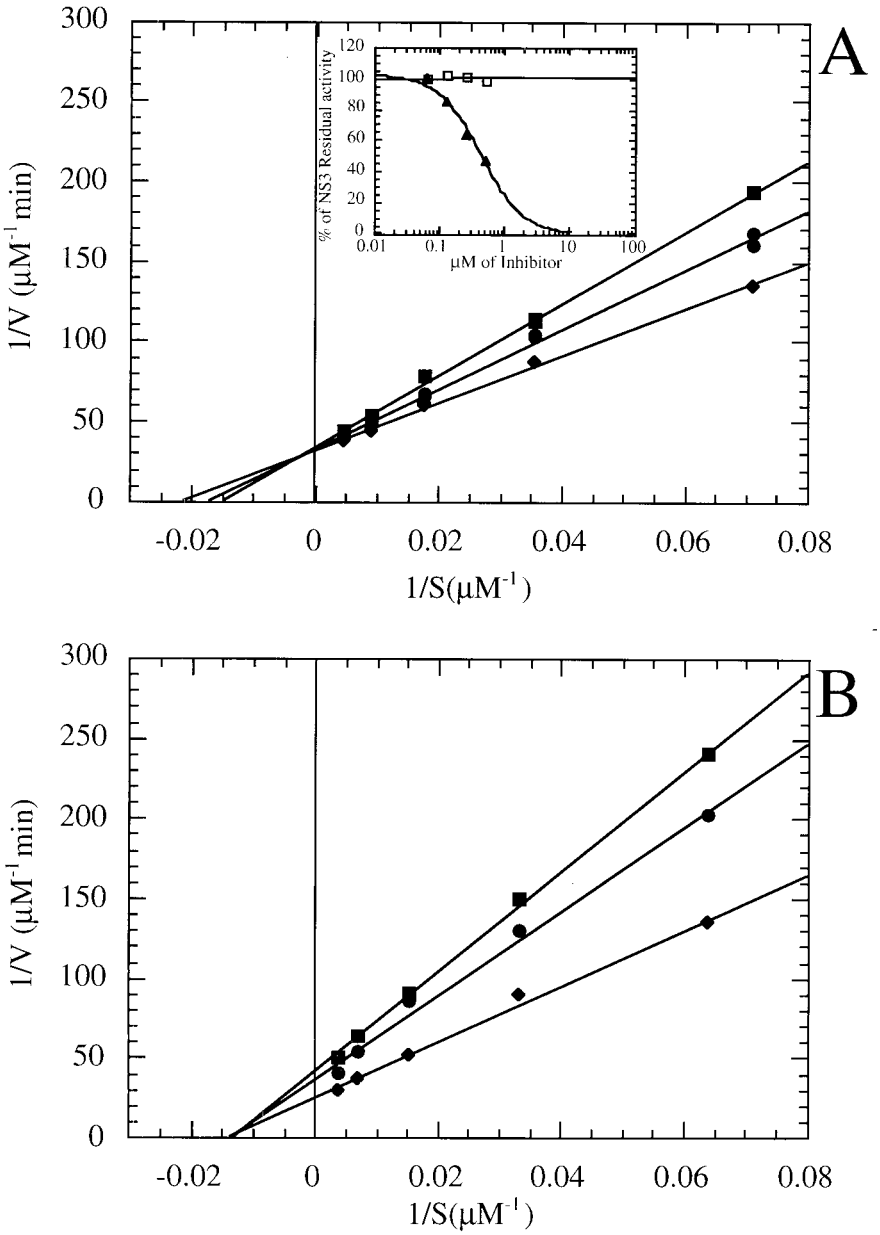

FIG. 7. Mechanism of inhibition of NS3 protease activity by hPSTI and MBip. Recombinant NS3 protease activity was determined at 25°C in 50 mM Tris (pH 7.5)–30 mM DTT–3 μM NS4A peptide–2% CHAPS–50% glycerol (for MBip) or in 1% CHAPS–15% glycerol–0.1 mM DTT (for hPSTI-C3). (A) Double-reciprocal plot of NS3 inhibition by hPSTI. Substrate titration curves were recorded in the absence of hPSTI (diamonds) and in the presence of 0.78 μM (circles) and 1.56 μM (squares) hPSTI. In the inset is shown the activity of hPSTI-C3 before (triangles) and after (squares) treatment with iodoacetamide; the experiment was carried out as described in the legend to Fig. 5 (*y* axis, residual enzyme activity; *x* axis, protein concentration). (B) Double-reciprocal plot of NS3 inhibition by MBip. Substrate titration curves were recorded in the absence of MBip (diamonds) and in the presence of 1.5 μM (circles) and 3 μM (squares) MBip.

tallization and biochemical studies are needed before a substantial step forward in the development of effective NS3 protease inhibitors can be made.

The rationale for focusing our study on two distinct macromolecules was twofold. The minibody (29, 33) is a "minimized" (5, 25) antibody-like protein that was chosen because, as for natural small-polyprotein scaffolds (32), it has emerged as a means of generating conformationally defined structures with potential as pharmacophores (38, 48). In addition, antibody fragments have been recently shown to be suitable macromolecules for generating NS3 protease inhibitors (31). The reason for choosing the Kazal-type inhibitor hPSTI stemmed from previous work which demonstrated that it was possible to isolate new specificities by displaying variants of natural protease inhibitors such as BPTI (35), ecotin (46), APPI (10), hPSTI (36), and LACI-D1 (27, 28) on phage.

The main conclusion of this study was that Kazal-type folds are suitable for producing NS3 competitive inhibitors, suggesting that a substrate-like "canonical" inhibition (4, 24) by a small proteinaceous inhibitor would also apply with the NS3 protease. In addition, because an unconstrained peptide corresponding to the amino acid sequence of hPSTI-C3 variable region was inactive (not shown), it appears that the rigidity of the main chain of the inhibitor binding loop is crucial in achiev-

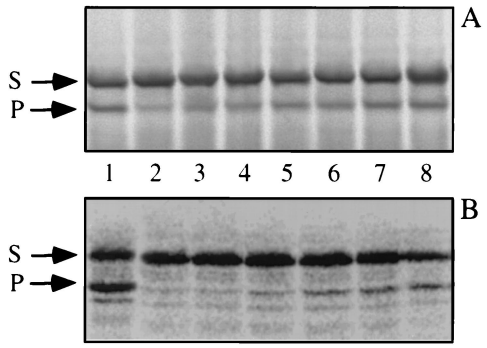

FIG. 8. In vitro-translated 70-kDa NS3 inhibition assay. Unlabelled full-length NS3 (70-kDa fragment) and [^{35}S]methionine-labelled NS5A/B substrate genes were transcribed in vitro by using T7 polymerase and translated in reticulocyte lysate. Lanes 2 to 7, decreasing amounts of purified hPSTI-C3 protein (1 to 5 μM) (A) and of MBip (0.6 to 20 μM) (B) were preincubated with the protease and NS4A cofactor (16 μM). Subsequently, the substrate (S) was added and incubated further, allowing conversion to occur. The percentage of cleaved substrate (P) was determined by densitometric analysis of the radiolabelled product after separation by SDS-PAGE. Lanes 1, no inhibitors.

ing effective enzyme inhibition. However, the potency (K_i = 360 nM) of this first-generation inhibitor is modest compared to the subnanomolar K_i values reported by others using different target proteases (10, 27, 28). This difference could reflect the limited complexity of the repertoire that was used, although our source was the same as that reported previously (36); however, we are eager to believe that it is rather a property of the enzyme, as also supported by biochemical (45) and structural (22) data. Affinity maturation studies will be required to clarify this issue. The minibody repertoire, on the other hand, yielded only one noncompetitive inhibitor that probably binds to an allosteric site (see below). We believe that the failure to find a competitive inhibitor was in this case due to the low complexity of the repertoire sampled (5×10^7) and to the limited number of clones characterized. This view is supported by the successful construction (relying on a noncombinatorial strategy, by grafting substrate sequences into the H2 loop) of a competitive minibody inhibitor of NS3 (our unpublished data).

The sequences of hPSTI variants selected show some interesting features, in particular the high frequency of cysteine residues found in the selected clones, albeit not always at the putative P1 position. This finding may reflect the substrate specificity of NS3, with a preference for Cys as the P1 residue. It should be stressed that the cysteine residue of hPSTI-C3 is crucial to its activity, since when it is modified by carboxyamidomethylation, the inhibitor loses its ability to block NS3 protease activity. In addition, cleavage of this molecule was not detectable even after incubation with high concentrations of enzyme for a long period of time.

Only a small fraction of the selected hPSTI variants (2 of 10) yielded detectable levels of expression in the periplasm of *E. coli*, which may be a consequence of the presence of unpaired cysteine residues in the variable region of some selected molecules, which may affect proper pairing of the native cysteine cross-linkages and hence allow the molecule to achieve native-like folding. Nonetheless, one of the two proteins purified from *E. coli* turned out to be a competitive inhibitor. It should be noted that most of the protein variants enriched after several rounds of selection were detectable by Western blotting of phage preparations as pIII fusions. One of the main difficulties that remains to be overcome is the establishment of expression systems that allow high levels of expression of these disulfide-rich small proteins in order to permit large-scale purification for X-ray or nuclear magnetic resonance spectroscopy studies. In the absence of X-ray studies of cocrystals, we can envision the use of modelling techniques to derive three-dimensional queries for searching databases of chemical collections using the modelled protease binding loop of hPSTI-C3 as a template.

Some conclusions can also be drawn for the minibody inhibitor, MBip. This is a selected variant of a de novo-designed β-pleated protein scaffold (a minimized antibody variable domain) which shows antiproteolytic activity with a moderate potency (IC_{50} = 1.5 μM). This value, however, was determined under optimal conditions for enzyme activity in vitro, which entails the inclusion in the assay of 50% glycerol. For the selection we used a lower glycerol concentration to ensure adequate binding affinity between epitope-tagged NS3 and its specific monoclonal antibody and also to take advantage of potential hydrophobically driven ligand-target interactions. By performing binding experiments with the protease with a lower glycerol concentration (15%), we estimated an apparent K_d of 75 to 150 nM in a direct binding assay (data not shown), indicating that it is possible to obtain minibody ligands with affinities equal to or lower than the previously observed limit of 200 nM (30) even from a nonoptimized ligand. The lack of a consensus sequence in this case is due to the limited complexity of the repertoire and the few selection steps carried out (two rather than four or five for hPSTI). The reason for limiting the number of affinity selection steps was mainly the fact that by increasing the number of rounds, we observed overgrowth of faulty phage clones. This inconvenience is likely to be linked to the nature of the display format (phage rather than phagemid), where all copies of pIII are modified and thus some variants may affect phage infectivity. In contrast, this problem is not as marked in the phagemid format. It must be stressed that the inhibition mechanism of MBip is noncompetitive, presumably as a result of binding to a site different from that of the substrate. By binding to this secondary site, MBip may alter the enzyme structure, thus affecting catalytic activity in a noncompetitive fashion. This secondary allosteric binding site is also distinct from the site where the cofactor NS4A binds, as the inhibition activity is unaffected by its presence, and it may be the binding site for another virally encoded or host factor(s).

NS3 is part of a large polyprotein and associates with other virally encoded protein domains; thus, it is important to characterize these functional sites, which could constitute targets for protein-protein interaction inhibitors. The NS3 minibody ligands may well be useful molecules for interfering with viral assembly, as they could inhibit interactions between NS3 and other uncharacterized viral or host factors. Unfortunately, the lack of a biological assay currently hampers these experiments.

ACKNOWLEDGMENTS

N.D. and F.M. contributed equally to this work.

We are grateful to P. Röttgen for the kind gift of the hPSTI expression vector (pMAC8). We also thank our colleagues V. Matassa, A. Tramontano, C. Traboni, and N. La Monica for valuable discussions, A. Lahm for help with the molecular graphics, P. Delmastro for the gift of purified monoclonal antibody 9E10, P. Neuner for the synthesis of oligonucleotides, A. Pessi and S. Acali for peptide synthesis, M. Ceretani and S. Serafini for assistance with the elastase and kallikrein assays, B. McManus and J. Clench for revision of the manuscript, and M. Emili for art graphics.

REFERENCES

1. **Ausubel, F. M., R. Brent, R. E. Kingston, D. D. Moore, J. G. Seidman, J. A. Smith, and K. Struhl.** 1994. Current protocols in molecular biology, vol. I

and II. Greene Publishing Associates, New York, N.Y.
2. **Bartenschlager, R., L. Ahlborn-Laake, J. Mous, and H. Jacobsen.** 1993. Nonstructural protein 3 of the hepatitis C virus encodes a serine-type proteinase required for cleavage at the NS3/4 and NS4/5 junctions. J. Virol. **67:**3835–3844.
3. **Bianchi, E., S. Venturini, A. Pessi, A. Tramontano, and M. Sollazzo.** 1994. High level expression and rational mutagenesis of a designed protein, the minibody: from an insoluble to a soluble molecule. J. Mol. Biol. **236:**649–659.
4. **Bode, W., and R. Huber.** 1992. Natural protein proteinase inhibitors and their interaction with proteinases. Eur. J. Biochem. **204:**433–451.
5. **Braisted, A. C., and J. A. Wells.** 1996. Minimizing a binding domain from protein A. Proc. Natl. Acad. Sci. USA **93:**5688–5692.
6. **Chambers, T. J., R. C. Weir, A. Grakoui, D. W. McCourt, F. F. Bazan, R. J. Fletterick, and C. M. Rice.** 1990. Evidence that the N-terminal domain of nonstructural protein NS3 from yellow fever virus is a serine protease responsible for site-specific cleavages in the viral polyprotein. Proc. Natl. Acad. Sci. USA **87:**8898–8902.
7. **Chien, D., Q. L. Choo, A. Tabrizi, C. Kuo, J. McFarland, K. Berger, C. Lee, J. Shuster, T. Nguyen, D. Moyer, M. M. Tong, S. Furuta, M. Omata, G. Tegtmeyer, H. Alter, E. Schiff, L. Jeffers, M. Houghton, and G. Kuo.** 1992. Diagnosis of hepatitis C virus (HCV) infection using an immunodominant chimeric polyprotein to capture circulating antibodies: reevaluation of the role of HCV in liver disease. Proc. Natl. Acad. Sci. USA **89:**10011–10015.
8. **Choo, Q. L., G. Kuo, A. J. Weiner, L. R. Overby, D. W. Bradley, and M. Houghton.** 1989. Isolation of a cDNA clone derived from a blood-borne non-A, non-B viral hepatitis genome. Science **244:**359–362.
9. **Choo, Q. L., K. H. Richman, J. H. Ham, K. Berger, C. Lee, C. Dong, C. Gallegos, D. Coit, A. Medina-Selby, P. J. Barr, A. J. Weiner, D. W. Bradley, G. Kuo, and M. Houghton.** 1991. Genetic organization and diversity of the hepatitis C virus. Proc. Natl. Acad. Sci. USA **88:**2451–2455.
10. **Dennis, M. S., and R. A. Lazarus.** 1994. Kunitz domain inhibitor of tissue-factor VIIa. J. Biol. Chem. **269:**22137–22144.
11. **Eckart, M. R., M. Selby, F. Masiarz, C. Lee, K. Berger, K. Crawford, C. Kuo, G. Kuo, M. Houghton, and Q. L. Choo.** 1993. The hepatitis C virus encodes a serine protease involved in processing of the putative nonstructural proteins from the viral polyprotein precursor. Biochem. Biophys. Res. Commun. **192:**399–406.
12. **Failla, C., L. Tomei, and R. De Francesco.** 1995. An amino-terminal domain of the hepatitis C virus NS3 protease is essential for interaction with NS4A. J. Virol. **69:**1769–1777.
13. **Failla, C., E. Pizzi, R. De Francesco, and A. Tramontano.** 1996. Redesigning the substrate specificity of the hepatitis C virus NS3 protease. Folding Design **1:**35–42.
14. **Felici, F., L. Castagnoli, A. Musacchio, R. Jappelli, and G. Cesareni.** 1991. Selection of antibody ligands from a large library of oligopeptides expressed on a multivalent exposition vector. J. Mol. Biol. **222:**301–310.
15. **Grakoui, A., C. Wychowski, C. Lin, S. M. Feinstone, and C. M. Rice.** 1993. Expression and identification of hepatitis C virus polyprotein cleavage products. J. Virol. **67:**1385–1395.
16. **Grakoui, A., D. W. McCourt, C. Wychowski, S. M. Feinstone, and C. M. Rice.** 1993. Characterization of the hepatitis C virus-encoded serine proteinase: determination of proteinase-dependent polyprotein cleavage sites. J. Virol. **67:**2832–2843.
17. **Hijikata, M., N. Kato, Y. Ootusyama, M. Nakagawa, and K. Shimotohno.** 1991. Gene mapping of the putative structural region of the hepatitis C virus genome by in vitro processing analysis. Proc. Natl. Acad. Sci. USA **88:**5547–5551.
18. **Hochuli, E., D. Gillessen, and H. P. Kocher.** 1987. Specificity of the immunoadsorbent used for large-scale recovery of interferon alpha-2a. J. Chromatogr. **411:**371–378.
19. **Jappelli, R., A. Luzzago, P. Tataseo, I. Pernice, and G. Cesareni.** 1992. Loop mutations can cause a substantial conformational change in the carboxy terminus of the ferritin protein. J. Mol. Biol. **227:**532–543.
20. **Kato, M., M. Hijikata, Y. Ootsuyama, M. Nakagawa, S. Ohkoshi, T. Sugimura, and K. Shimotohno.** 1990. Molecular cloning of human hepatitis C virus genome from Japanese patients with non-A, non-B hepatitis. Proc. Natl. Acad. Sci. USA **87:**9524–9528.
21. **Kim, D. W., Y. Gwack, J. H. Han, and J. Choe.** 1995. C-terminal domain of the hepatitis C virus NS3 protein contains an RNA helicase activity. Biochem. Biophys. Res. Commun. **215:**160–166.
22. **Kim, J. L., K. A. Morgenstern, C. Lin, T. Fox, M. D. Dwyer, J. A. Landro, S. P. Chambers, W. Markland, C. A. Lepre, E. T. O'Malley, S. L. Harbeson, C. M. Rice, M. A. Murcko, P. R. Caron, and J. A. Thomson.** 1996. Crystal structure of the hepatitis C virus NS3 protease domain complexed with a synthetic NS4A cofactor peptide. Cell **87:**343–355.
23. **Kuo, G., Q. L. Choo, H. J. Alter, G. L. Gitnick, A. G. Redecker, R. H. Purcell, T. Myamura, J. L. Dienstag, M. J. Alter, C. E. Syevens, G. E. Tagtmeyer, F. Bonino, M. Colombo, W. S. Lee, C. Kuo, K. Berger, J. R. Shister, L. R. Overby, D. W. Bradley, and M. Houghton.** 1989. An assay for circulating antibodies to a major etiologic virus of human non-A, non-B hepatitis. Science **244:**362–364.
24. **Laskowski, M., Jr., and I. Kato.** 1980. Protein inhibitors of proteinases. Annu. Rev. Biochem. **49:**593–626.
25. **Li, B., J. Y. Tom, D. Oare, R. Yen, W. J. Fairbrother, J. A. Wells, and B. C. Cunningham.** 1995. Minimization of a polypeptide hormone. Science **270:**1657–1660.
26. **Love, R. A., H. E. Parge, J. A. Wickersham, Z. Hostomsky, N. Habuka, E. W. Moomaw, T. Adachi, and Z. Hostomska.** 1996. The crystal structure of hepatitis C virus NS3 proteinase reveals a trypsin-like fold and a structural zinc binding site. Cell **87:**331–342.
27. **Markland, W., A. C. Ley, S. W. Lee, and R. C. Ladner.** 1996. Iterative optimization of high-affinity protease inhibitors using phage display. 1. Plasmin. Biochemistry **35:**8045–8057.
28. **Markland, W., A. C. Ley, and R. C. Ladner.** 1996. Iterative optimization of high-affinity protease inhibitors using phage display. 2. Plasma kallikrein and thrombin. Biochemistry **35:**8058–8067.
29. **Martin, F., C. Toniatti, A. L. Salvati, S. Venturini, G. Ciliberto, R. Cortese, and M. Sollazzo.** 1994. The affinity-selection of a minibody polypeptide inhibitor of human interleukin-6. EMBO J. **13:**5303–5309.
30. **Martin, F., C. Toniatti, A. L. Salvati, G. Ciliberto, R. Cortese, and M. Sollazzo.** 1996. Coupling protein design and in vitro selection strategies: improving specificity and affinity of a designed β-protein IL-6 antagonist. J. Mol. Biol. **255:**86–97.
31. **Martin, F., C. Volpari, C. Steinkühler, N. Dimasi, M. Brunetti, G. Biasiol, S. Altamura, R. Cortese, R. De Francesco, and M. Sollazzo.** 1997. Affinity-selection of a *camelized* V_H domain antibody inhibitor of Hepatitis C Virus NS3 protease. Prot. Eng. **10:**607–614.
32. **McConnell, S. J., and R. H., Hoess.** 1995. Tendamistat as a scaffold for conformationally constrained phage peptide libraries. J. Mol. Biol. **250:**460–470.
33. **Pessi, A., E. Bianchi, A. Crameri, S. Venturini, A. Tramontano, and M. Sollazzo.** 1993. A designed metal-binding protein with a novel fold. Nature (London) **362:**367–369.
34. **Pizzi, E., A. Tramontano, L. Tomei, N. La Monica, C. Failla, M. Sardana, T. Wood, and R. De Francesco.** 1994. Molecular model of the specificity pocket of the hepatitis C virus protease: implication for substrate recognition. Proc. Natl. Acad. Sci. USA **91:**888–892.
35. **Roberts, B. L., W. Markland, A. C. Ley, R. B. Kent, D. W. White, S. K. Guterman, and R. C. Ladner.** 1992. Directed evolution of a protein: selection of potent neutrophil elastase inhibitors displayed on M13 fusion phage. Proc. Natl. Acad. Sci. USA **89:**2429–2433.
36. **Röttgen, P., and J. Collins.** 1995. A human pancreatic secretory trypsin inhibitor presenting a hypervariable highly constrained epitope via monovalent phagemid display. Gene **164:**243–250.
37. **Smith, G. P.** 1985. Filamentous fusion phage: novel expression vectors that display cloned antigens on the virion surface. Science **228:**1315–1317.
38. **Sollazzo, M., E. Bianchi, F. Felici, R. Cortese, and A. Pessi.** 1995. Conformationally defined peptide libraries on phage: selectable templates for the design of pharmacological agents, p. 127–143. *In* R. Cortese (ed.), Combinatorial libraries. de Gruyter, Berlin, Germany.
39. **Steinkühler, C., L. Tomei, and R. De Francesco.** 1996. *In vitro* activity of hepatitis C virus protease NS3 purified from recombinant baculovirus-infected Sf9 cells. J. Biol. Chem. **271:**6367–6373.
40. **Steinkühler, C., A. Urbani, L. Tomei, G. Biasiol, M. Sardana, E. Bianchi, A. Pessi, and R. De Francesco.** 1996. Activity of purified hepatitis C virus protease NS3 on peptide substrates. J. Virol. **70:**6694–6700.
41. **Szardening, M., and J. Collins.** 1990. A phasmid optimised for protein design projects: pMAFMPF. Gene **94:**1–7.
42. **Takamizawa, A., C. Mori, I. Fuke, S. Manabe, S. Murakami, J. Fujita, J. E. Onoshi, T. Andoh, I. Yoshida, and H. Okayama.** 1991. Structure and organization of the hepatitis C virus genome isolated from human carriers. J. Virol. **65:**1105–1113.
43. **Tomei, L., C. Failla, E. Santolini, R. De Francesco, and N. La Monica.** 1993. NS3 is a serine protease required for processing of hepatitis C virus polyprotein. J. Virol. **67:**4017–4026.
44. **Tomei, L., C. Failla, R. L. Vitale, E. Bianchi, and R. De Francesco.** 1996. A central hydrophobic domain of the hepatitis C virus NS4A protein is necessary and sufficient for the activation of the NS3 protease. J. Gen. Virol. **77:**1065–1070.
45. **Urbani, A., E. Bianchi, F. Narjes, A. Tramontano, R. De Francesco, C. Steinkühler, and A. Pessi.** 1997. Substrate specificity of the Hepatitis C Virus serine protease NS3. J. Biol. Chem. **272:**9204–9209.
46. **Wang, C. I., Q. Yang, and C. S. Craik.** 1995. Isolation of a high affinity inhibitor of urokinase-type plasminogen activator by phage display of ecotin. J. Biol. Chem. **270:**12250–12256.
47. **Weiland, O.** 1994. Interferon therapy in chronic hepatitis C virus infection. FEMS Microbiol. Rev. **14:**279–288.
48. **Zhao, B., L. R. Helms, R. L. DesJarlais, S. S. Abdel-Meguid, and R. Wetzel.** 1995. A paradigm for drug discovery using a conformation from the crystal structure of a presentation scaffold. Nat. Struct. Biol. **2:**1131–1137.